



THE UNIVERSITY *of* EDINBURGH

## Edinburgh Research Explorer

# Optimal low-carbon economic environmental dispatch of hybrid electricity-natural gas energy systems considering P2G

### Citation for published version:

Liu, J, Sun, W & Harrison, G 2019, 'Optimal low-carbon economic environmental dispatch of hybrid electricity-natural gas energy systems considering P2G', *Energies*, vol. 12, no. 7, 1355.  
<https://doi.org/10.3390/en12071355>

### Digital Object Identifier (DOI):

[10.3390/en12071355](https://doi.org/10.3390/en12071355)

### Link:

[Link to publication record in Edinburgh Research Explorer](#)

### Document Version:

Peer reviewed version

### Published In:

Energies

### Publisher Rights Statement:

© 2019 by the authors. Licensee MDPI, Basel, Switzerland. This article is an open access article distributed under the terms and conditions of the Creative Commons Attribution (CC BY) license (<http://creativecommons.org/licenses/by/4.0/>).

### General rights

Copyright for the publications made accessible via the Edinburgh Research Explorer is retained by the author(s) and / or other copyright owners and it is a condition of accessing these publications that users recognise and abide by the legal requirements associated with these rights.

### Take down policy

The University of Edinburgh has made every reasonable effort to ensure that Edinburgh Research Explorer content complies with UK legislation. If you believe that the public display of this file breaches copyright please contact [openaccess@ed.ac.uk](mailto:openaccess@ed.ac.uk) providing details, and we will remove access to the work immediately and investigate your claim.



1 Article

# 2 Optimal low-carbon economic environmental 3 dispatch of hybrid electricity-natural gas energy 4 systems considering P2G

5 Jing Liu <sup>1,\*</sup>, Wei Sun <sup>2</sup> and Gareth Harrison <sup>2</sup>

6 <sup>1</sup> School of Mechanical Electronic and Information Engineering, China University of Mining & Technology  
7 (Beijing), Beijing, 100083, China; jingqisandral@163.com

8 <sup>2</sup> School of Engineering, University of Edinburgh, Edinburgh, EH9 3DW, UK; W.Sun@ed.ac.uk (W. S.);  
9 Gareth.Harrison@ed.ac.uk (G.H.)

10 \* Correspondence: jingqisandral@163.com

11 Received: date; Accepted: date; Published: date

12 **Abstract:** Power to gas facilities (P2G) could absorb excess renewable energy that would otherwise  
13 be curtailed due to electricity network constraint by converting it to methane (synthetic natural  
14 gas). The produced synthetic natural gas can power gas turbines and realize bidirectional energy  
15 flow between power and natural-gas system. P2G therefore has significantly potential of unlocking  
16 inherent flexibility of the integrated system, but also pose new challenges of increased system  
17 complexity. Coordinated operation strategy that manages power and natural-gas network  
18 constraints together is essential to address such challenge. In this paper, a novel low-carbon  
19 economic environmental dispatch strategy is presented considering all the constraints in both  
20 systems. The multi-objective black-hole particle swarm optimization algorithm (MOBHPSO) is  
21 adopted. In addition to P2G, gas demand management strategy is proposed to support gas flow  
22 balance. A new solving approach that combines effective redundancy method, trust region method  
23 and Levenberg-Marquardt method is proposed to address the complex coupled constraints. Case  
24 studies that use integrated IEEE 39-bus power and Belgian high-calorific 20-node gas system  
25 demonstrate the effectiveness and scalability of the proposed model and optimization method. The  
26 analysis of dispatch results illustrates the benefit of P2G in the wind power accommodation,  
27 low-carbon, economic and environmental improvement of integrated system operation.

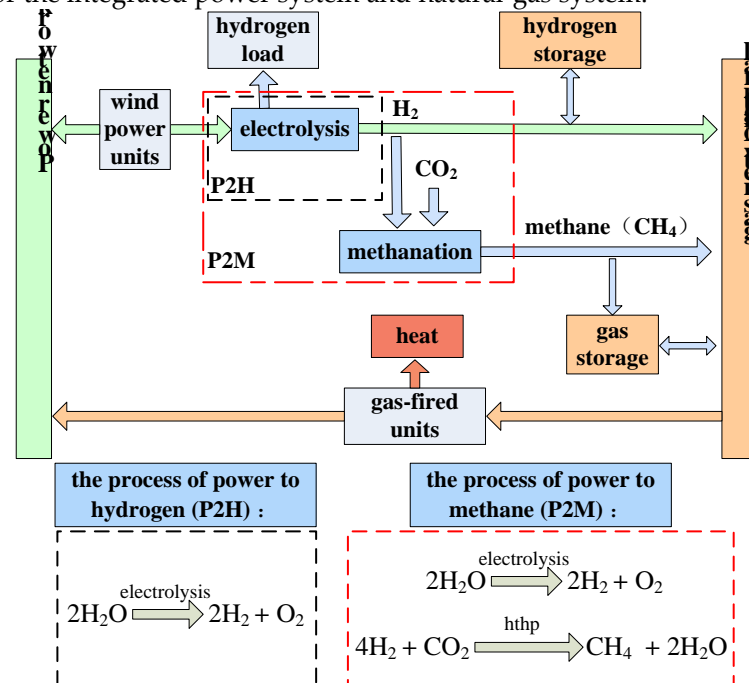
28 **Keywords:** hybrid electricity-natural gas energy systems; power to gas (P2G); low-carbon;  
29 economic environmental dispatch; trust region method; Levenberg-Marquardt method  
30

## 31 1. Introduction

32 With further acceleration of the low-carbon energy process, as well as the energy crisis,  
33 environmental pollution and other issues, the capacity of renewable energy sources is increased  
34 continuously. While, due to the intermittency and uncertainty of wind power as well as the lack of  
35 peak load regulation of power system, it is likely that more and more wind power generation will  
36 have to be curtailed in order to maintain the power system reliability [1]. To solve this problem,  
37 much research is carried out to explore practical means to reduce the curtailment of wind power  
38 generation. With the growing interdependence of power system and natural-gas system and the  
39 development of power to gas technologies [2-8], it creates operational interactions between power  
40 system and natural-gas system which could obtain additional benefits for both systems including  
41 reducing the curtailed wind power generation. On the one hand, the power system tends to require  
42 more flexible power energy from the natural-gas system to shift peak load whereby the gas-fired

43 units [3], which is conducive to the accommodation of wind power. On the other hand, the  
 44 natural-gas system absorbs methane or hydrogen produced by P2G to guarantee the continuity of  
 45 gas supply and the wind power energy will be stored and transported in the existing natural-gas  
 46 system for generating low-carbon electricity or heat later [9-11], which uses the curtailed wind  
 47 power directly. Therefore, the integrated electricity-natural gas energy systems with P2G have  
 48 become one of the effective forms to reduce the curtailment of wind power generation.

49 The diagram of integrated electricity-natural gas energy systems with P2G is shown in Figure 1.  
 50 It can be seen that the power system and the natural-gas system exchange the energy whereby P2G  
 51 and gas-fired units. When the curtailed wind power is converted to hydrogen or methane whereby  
 52 power to hydrogen facilities (P2H) or power to methane facilities (P2M), P2G which includes P2H  
 53 and P2M is the load of power system and the gas source of natural-gas system. Meanwhile, the  
 54 gas-fired units are the load of natural-gas system and the generators of power system. Obviously,  
 55 operation parameters of P2G, power system and natural-gas system are interrelated and interactive  
 56 which can affect the operation cost, CO<sub>2</sub> emissions, reliability and stability of both systems.  
 57 Therefore, how to deal with the interactive relationship between power system and natural-gas  
 58 system and how to achieve coordinated optimal operation with economic environmental benefits  
 59 are the key issues for the integrated power system and natural-gas system.



60  
 61 **Figure 1.** Diagram of integrated electricity and natural-gas energy systems with P2G

62 For the integrated electricity-natural gas energy systems, the initial research is focused on  
 63 optimal power flow [12-15], unit commitment [16], optimal dispatch [17-19] and steady-state  
 64 analysis [20] and system planning [21]. For the calculation of optimal power flow, the total operation  
 65 cost is usually considered as optimal objective and the dual interior point method [12], the Monte  
 66 Carlo method [13], the point estimation method [14] are adopted frequently. Some studies introduce  
 67 energy hub to deal with the translation of different energies in the hybrid electricity-natural gas  
 68 energy systems [13,17]. For the optimization of system operation, the operation of power system and  
 69 the operation of natural-gas system are mostly optimized separately using the deterministic  
 70 optimization methods or stochastic optimization methods [18]. For the steady-state analysis of the  
 71 hybrid electricity-natural gas energy systems, basing on the steady-state analysis of power system,  
 72 the analysis model of natural-gas system is realized by analogy analysis between power system and  
 73 natural-gas system, and then the comprehensive steady-state analysis model of hybrid  
 74 electricity-natural gas energy systems is given [20]. For the optimal system planning, a chance  
 75 constrained programming approach is presented to minimize the investment cost of the integrated  
 76 energy systems [21]. In these studies, P2G is not considered. While, as the coupling operation link of  
 77 the power system and natural-gas system, P2G plays a more and more important role in wind power

78 accommodation with broad prospects and potential for energy development [22-24]. Therefore, it is  
79 necessary to carry out the research on optimal operation of integrated electricity-natural gas energy  
80 systems considering P2G. The early studies on P2G are mainly focused on technology  
81 implementation and security application [6, 25-28]. Recently, although some achievements about  
82 optimal operation of integrated electricity-natural gas energy systems considering P2G have been  
83 achieved [6-8, 24,29-38], it still seems to be in the exploratory stage from the following aspects.

84 (1) Optimal objectives: The minimum total operation cost is mostly adopted [6, 24,29-32,37].  
85 Only in a few studies, the maximum wind power accommodation [33] or the minimum energy  
86 purchase cost [34] or net power demand smoothness [38] is also considered as the objective. While,  
87 environmental benefit is rarely considered. As we know, the low-carbon and emission reduction  
88 requirements become more and more important. So it is necessary to take environmental benefit  
89 into consideration.

90 (2) Optimal models: The operation model of power system and operation model of natural-gas  
91 system are mainly established separately basing on the two-level optimal power flow structure [6,  
92 30-32]. It seems that rare consideration is given to coordinated optimization between the two energy  
93 systems.

94 (3) Optimal algorithms: Generally, the traditional algorithms are adopted in most studies, such  
95 as mix-integer linear programming method [3,24], mixed-integer quadratic programming method  
96 [37] and interior point method [35]. While, the intelligent optimization algorithms with high global  
97 search ability and fast convergence speed are rarely used.

98 (4) Constraints handling methods: The constraints handling methods affect the operation  
99 results directly. While, few articles give full details about the constraints handling methods,  
100 especially for the complicated dynamic nodal balance constraint and volume limits of gas storage in  
101 the natural-gas system.

102 On the above premises, this paper establishes the optimal operation model of the hybrid  
103 electricity-natural gas energy systems considering operation cost, natural-gas cost reduction due to  
104 P2G, CO<sub>2</sub> emissions and SO<sub>x</sub> emissions to achieve low-carbon, economic and environmental benefits.  
105 The multi-objective black-hole particle swarm optimization algorithm (MOBHPSO) [39-42] is  
106 adopted. The power flow is calculated using Newton-Raphson method. And the non-linear gas flow  
107 equations are solved by trust region method [43-44] and Levenberg-Marquardt (L-M) method  
108 [45-46], respectively. The gas demand management strategy is proposed to balance the gas flow.  
109 Moreover, the detailed handling methods of inequality constraints in natural-gas system are also  
110 given in this paper. Several case studies are carried out on a hybrid IEEE 39-bus power system and  
111 Belgian high-calorific 20-node gas system in a period of 24 hours to investigate the low-carbon,  
112 economic and environmental benefits of P2G in terms of cost reduction (6.165×10<sup>5</sup>\$), rate decline of  
113 wind curtailment (from 24.85% to 4.04%), CO<sub>2</sub> emissions reduction (3630 ton) and SO<sub>x</sub> emissions  
114 reduction (0.254 ton).

## 115 2. Problem Formulation

116 The optimal low-carbon economic environmental dispatch problem of hybrid  
117 electricity-natural gas energy systems with P2G is a complicated non-convex, coupled, non-linear,  
118 multi-objective and multi-constraint optimization problem. It contains three parts: the first one is the  
119 optimization of power system; the second one is the optimization of natural-gas system; and the last  
120 one is the coordination of the hybrid electricity-natural gas energy systems. The flow chart of this  
121 optimization problem is shown in Figure 2. Each part of the flow chart will be described in details.

### 122 2.1 Optimal economic environmental dispatch of power system

#### 123 2.1.1 Objectives

$$\text{Min } F_p = \sum_{i=1}^{N_G} \sum_{t=1}^T a_i P_{Gi}(t)^2 + b_i P_{Gi}(t) + c_i \tag{1}$$

$$\text{Min } E_{SO_x} = \sum_{i=1}^{N_G} \sum_{t=1}^T (\alpha_i + \beta_i P_{Gi}(t) + \gamma_i P_{Gi}(t)^2 + \delta_i e^{\lambda_i P_{Gi}(t)}) \tag{2}$$

$$\text{Min } L_p = \frac{\sum_{t=1}^T \left[ P_L(t) + \sum_{k=1}^{N_{P2G}} P_{P2G,k}(t) - \sum_{i=1}^{N_G} P_{Gi}(t) \right]}{\sum_{t=1}^T P_L(t)} \tag{3}$$

124 Where  $F_p$  is the fuel cost of power system;  $N_G$  is the number of power generations;  $T$  is the  
 125 number of time periods;  $P_{Gi}(t)$  is the power generation output at time  $t$ ;  $a_i, b_i, c_i$  are coefficient of the  
 126 fuel cost;  $E_{SO_x}$  is the pollutant emission of  $SO_x$ ;  $\alpha_i, \beta_i, \gamma_i, \delta_i, \lambda_i$  are coefficient of the pollutant emission;  
 127  $L_p$  is the load loss rate presenting the reliability of power supply;  $N_{P2G}$  is the number of P2G;  $P_L(t)$  is  
 128 the power load at time  $t$ ;  $P_{P2G}(t)$  is the power supplied to the P2G facilities at time  $t$ .

129 The power output of gas-fired units is calculated by the product of the gas flow injected to the  
 130 gas-fired units  $Q_{GT}(t)$ , higher heating value of natural gas  $HHV_g$  and the energy conversion efficiency  
 131  $\eta_{GT}(t)$ . In this paper, the last objective is converted into a constraint by being less than a given value  $\epsilon$ .

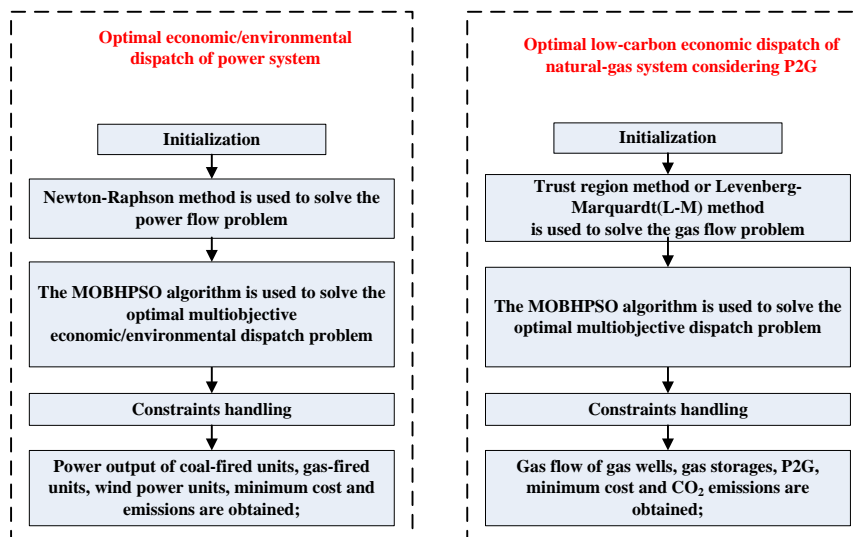
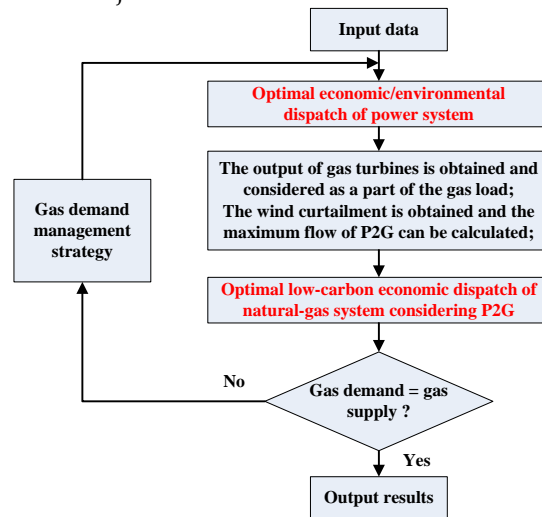


Figure 2. Flow chart

## 134 2.1.2 Constraints

## 135 (1) Power output limits

$$P_{Gi}^{\min} \leq P_{Gi}(t) \leq P_{Gi}^{\max} \quad (4)$$

136 Where  $P_{Gi}^{\min}$  and  $P_{Gi}^{\max}$  represent the minimum power output and maximum power output of  
137 unit  $i$ , respectively.

## 138 (2) Ramp rate limits

$$\begin{cases} P_{Gi}(t) \geq \max\{P_{Gi}^{\min}, P_{Gi}(t-1) - \Delta P_{Gi}^{\text{down}}\}, & P_{Gi}(t) \leq P_{Gi}(t-1) \\ P_{Gi}(t) \leq \min\{P_{Gi}^{\max}, P_{Gi}(t-1) + \Delta P_{Gi}^{\text{up}}\}, & P_{Gi}(t) \geq P_{Gi}(t-1) \end{cases} \quad (5)$$

139 Where  $\Delta P_{Gi}^{\text{up}}$  and  $\Delta P_{Gi}^{\text{down}}$  represent the ramp up rate and the ramp down rate of unit  $i$ ,  
140 respectively.

## 141 (3) Line capacity limit

$$S_l(t) \leq S_l^{\max} \quad (6)$$

142 Where  $S_l^{\max}$  is the maximum capacity of line  $l$ .

## 143 2.2 Optimal low-carbon economic dispatch of natural-gas system considering P2G

## 144 2.2.1 Objectives

## 145 (1) Minimum the operational cost of natural-gas system

$$\text{Min } C_{\text{well}} + C_{\text{gs}} + C_{\text{P2G}} - S_{\text{P2G}} \quad (7)$$

$$C_{\text{well}} = \sum_{n=1}^{N_w} \sum_{t=1}^T Q_{wn}(t) u_{wn}(t) \quad (8)$$

$$C_{\text{gs}} = \sum_{m=1}^{N_{\text{gs}}} \sum_{t=1}^T Q_{gs,m}(t) u_{gs,m}(t) \quad (9)$$

$$C_{\text{P2G}} = \sum_{k=1}^{N_{\text{P2G}}} \sum_{t=1}^T P_{\text{P2G},k}(t) u_{\text{P2G},k} \quad (10)$$

$$S_{\text{P2G}} = \sum_{k=1}^{N_{\text{P2G}}} \sum_{t=1}^T Q_{\text{P2G},k}(t) u_{\text{ave}}(t) \quad (11)$$

146 Where  $C_{\text{well}}$ ,  $C_{\text{gs}}$ ,  $C_{\text{P2G}}$  represent the operation cost of gas wells, the operation cost of gas storage,  
147 the operation cost of P2G, respectively.  $S_{\text{P2G}}$  is the saved natural-gas cost due to the P2G.  $N_w$ ,  $N_{\text{gs}}$   
148 represent the number of gas wells and the number of gas storage, respectively;  $Q_{wn}(t)$  is the gas flow  
149 of gas well  $n$ ;  $u_{wn}(t)$  is the gas price of gas well  $n$  at time  $t$ ;  $Q_{gs,m}(t)$  is the gas flow of gas storage  $m$   
150 at time  $t$  (It is positive for inflow and negative for outflow);  $u_{gs,m}(t)$  is the storage price for gas storage  $m$   
151 at time  $t$ ;  $u_{\text{P2G},k}$  is the operation cost of P2G  $k$ ;  $Q_{\text{P2G},k}(t)$  is the gas flow of P2G  $k$  at time  $t$ ;  $u_{\text{ave}}(t)$  is the  
152 average gas price (In this paper, it is the average price of gas wells).

153 (2) Minimum the CO<sub>2</sub> emissions of the natural-gas system

$$\text{Min } E_{CO_2} = \sum_{n=1}^{N_w} \sum_{t=1}^T E_{wn}(t) + \sum_{m=1}^{N_{gs}} \sum_{t=1}^T E_{gs,m}(t) - \sum_{k=1}^{N_{P2G}} \sum_{t=1}^T E_{P2G,k}(t) \quad (12)$$

154 Where  $E_{CO_2}$  represents CO<sub>2</sub> emissions of the natural-gas system;  $E_{wn}(t)$ ,  $E_{gs,m}(t)$  are the CO<sub>2</sub>  
 155 emissions of gas well  $n$ , gas storage  $m$  at time  $t$ , respectively;  $E_{P2G,k}(t)$  is the amount of CO<sub>2</sub> absorbed  
 156 by the methanation process of P2G  $k$  at time  $t$ .

## 157 2.2.2 Constraints

### 158 (1) Gas flow limits of gas wells

$$Q_{wn}^{\min} \leq Q_{wn}(t) \leq Q_{wn}^{\max} \quad (13)$$

159 Where  $Q_{wn}^{\min}$ ,  $Q_{wn}^{\max}$  represent the minimum gas flow and the maximum gas flow of gas well  $n$ ,  
 160 respectively.

### 161 (2) Gas pressure limits of gas nodes

$$M_i^{\min} \leq M_i(t) \leq M_i^{\max} \quad (14)$$

162 Where  $M_i(t)$  represents gas pressure of gas node  $i$  at time  $t$ .  $M_i^{\min}$  and  $M_i^{\max}$  are the minimum  
 163 and maximum gas pressure of gas node  $i$ .

### 164 (3) Gas flow equation of pipelines

165 The natural-gas system satisfies the mass conservation law of fluid dynamics and Bernoulli  
 166 equation in the operation. The relationship between gas flow of pipelines and gas pressure of gas  
 167 nodes can be modeled as follows [12, 35].

$$Q_{ij}(t) |Q_{ij}(t)| = C_{ij} (M_i(t)^2 - M_j(t)^2) \quad (15)$$

$$Q_{ij}(t) = \frac{Q_{ij}^{in}(t) + Q_{ij}^{out}(t)}{2} \quad (16)$$

168 Where  $Q_{ij}(t)$  is the average gas flow of pipeline  $ij$  (Pipeline  $ij$  is the pipeline between gas node  $i$   
 169 and gas node  $j$ );  $Q_{ij}^{in}(t)$  and  $Q_{ij}^{out}(t)$  are the injection and withdrawal gas flow of pipeline  $ij$ ,  
 170 respectively;  $C_{ij}$  is a constant related to the length, diameter, temperature and compressibility factor  
 171 of pipeline  $ij$ .

### 172 (4) Line pack equation

173 Due to the compressibility of natural gas, the injection gas flow and the withdrawal gas flow of  
 174 the same pipeline would be different. Some excess natural gas can be stored in the pipelines, which  
 175 is called line pack. The line pack of pipeline  $ij$  is related to the average pressure and its own  
 176 parameters of pipelines, which can be modeled as below [12,15].

$$L_{ij}(t) = \omega_{ij} M_{ij}(t) \quad (17)$$

$$M_{ij}(t) = \frac{M_i(t) + M_j(t)}{2} \quad (18)$$

$$L_{ij}(t) = L_{ij}(t-1) + Q_{ij}^{in}(t) - Q_{ij}^{out}(t) \quad (19)$$

177 Where  $L_{ij}(t)$  is the line pack of pipeline  $ij$  at time  $t$ ;  $\omega_{ij}$  is a constant related to pipeline parameters,  
 178 gas constant, compressibility factor, gas density and gas temperature.

179 (5) Nodal gas flow balance equation

180 For each gas node, the gas flows into the node must equals the gas flows out of the node.

$$\begin{aligned} & \sum_{n \in i} Q_{wn}(t) + \sum_{m \in i} Q_{gs,m}(t) + \sum_{k \in i} Q_{P2G,k}(t) - \sum_{j \in Set\_I(i)} Q_{ij}^{in}(t) \\ & + \sum_{j \in Set\_O(i)} Q_{ij}^{out}(t) - Q_{GT,i}(t) - Q_{Li}(t) = 0 \end{aligned} \quad (20)$$

181 Where, the first three items are the gas flow of gas wells, gas storage and P2G located at gas  
 182 node  $i$  at time  $t$ , respectively;  $Q_{GT,i}(t)$  and  $Q_{Li}(t)$  indicate the gas flow injected to gas-fired units and the  
 183 gas load at gas node  $i$  at time  $t$ , respectively;  $Set\_I(i)$  is the set of pipeline  $ij$  which lets gas node  $i$  as  
 184 the input node;  $Set\_O(i)$  is the set of pipeline  $ij$  which lets gas node  $i$  as the output node.

185 (6) Gas flow limits and capacity limits of gas storage

$$Q_{gs,m}^{\min} \leq Q_{gs,m}(t) \leq Q_{gs,m}^{\max} \quad (21)$$

$$V_m^{\min} \leq V_m(t) \leq V_m^{\max} \quad (22)$$

$$V_m(t) = V_m(t-1) + Q_{gs,m}(t) \quad (23)$$

186 Where  $Q_{gs,m}^{\min}$  and  $Q_{gs,m}^{\max}$  are the minimum and maximum gas flow of gas storage  $m$ ,  
 187 respectively;  $V_m(t)$ ,  $V_m^{\min}$ ,  $V_m^{\max}$  are the capacity of gas storage  $m$  at time  $t$ , the minimum and maximum  
 188 capacity of gas storage  $m$ , respectively; When the gas is injected to the gas storage,  $Q_{gs,m}(t)$  is positive,  
 189 otherwise is negative.

190 (7) Compressor

191 The compressors are used to boost the pressure of the natural-gas network, which can help the  
 192 natural gas transporting to each gas load. In this paper, the energy consumed by the compressors is  
 193 calculated by using natural gas flow through the compressors. The consumed gas flow of  
 194 compressor  $r$ ,  $Q_{cr}^{consume}(t)$ , is calculated as presented below [15].

$$Q_{cr}^{consume}(t) = \beta_{cr} P_{cr}(t) \quad (24)$$

$$P_{cr}(t) = \frac{Q_{cr}(t)}{\eta_{cr} \cdot \tau} \cdot \left( \left( \frac{M_{or}(t)}{M_{ir}(t)} \right)^{\tau} - 1 \right) \quad (25)$$

195 Where  $\beta_{cr}$  is energy conversion coefficient of compressor  $r$ ;  $P_{cr}(t)$  is the consumed energy by  
 196 compressor  $r$ ;  $Q_{cr}(t)$  is the gas flow flowing through compressor  $r$  at time  $t$ ;  $\eta_{cr}$  is the efficiency of  
 197 compressor  $r$ ;  $\tau = (\alpha - 1)/\alpha$  and  $\alpha$  is variability index of compressors;  $M_{or}(t)$  and  $M_{ir}(t)$  are the pressure of  
 198 output node and input node of compressor  $r$ , respectively.

199 (8) Gas flow limit of P2G

$$Q_{P2G,k}^{\min} \leq Q_{P2G,k}(t) \leq Q_{P2G,k}^{\max} \quad (26)$$

200 Where  $Q_{P2G,k}^{\min}$  and  $Q_{P2G,k}^{\max}$  are the minimum and maximum gas flow of P2G  $k$ , respectively.

201 2.3 Gas demand management strategy to coordinate the two energy systems



202 When the pressure of some gas nodes is higher than the maximum pressure or lower than the  
 203 minimum pressure, which means the gas demand and the gas supply is not balanced on these gas  
 204 nodes, then the gas demand management strategy is used. The main idea is to adjust the gas flow of  
 205 gas turbines to achieve the gas demand balance, which means changing the power output of  
 206 gas-fired units. Then the power output of units in power system will be adjusted.

#### 207 2.4 Constraints handling methods

208 The constraints of power system are handled using the methods presented in [39]. And in this  
 209 paper, the constraints of natural-gas system are handled by the proposed method as shown below.

##### 210 2.4.1 Equality constraints handling method

211 In this paper, the set of non-linear constraints equations (15)-(20) of the natural-gas system are  
 212 solved by trust region algorithm [43-44] and Levenberg-Marquardt algorithm (L-M) [45-46]. Trust  
 213 region and L-M methods are both simple and powerful tools for solving systems of nonlinear  
 214 equations and large-scale optimization problems. They have the advantages of guaranteeing a  
 215 solution whenever it exists [43-46]. In this paper, trust region method and L-M method are used to  
 216 solve the gas flow non-linear equations, respectively. And the optimization results are compared in  
 217 the case studies.

##### 218 2.4.2 Inequality constraints handling method

219 For the inequality constraints (13)(14)(21)(22)(26), the gas flow is the minimum when it is lower  
 220 than the minimum value and the gas flow is the maximum when it is over the maximum value. For  
 221 the gas storage volume constraint, the effective redundancy method is proposed in this paper. The  
 222 details of this method are as below.

- 223 a) For gas storage  $m$  at time  $t$ ;
- 224 b) If  $V_m(t) \leq V_m^{\min}$ , calculate  $\Delta V = V_m^{\min} - V_m(t)$ ;
- 225 c) For  $ii = 1:t$ , calculate the gas flow redundancy of gas storage  $m$  at time  $ii$ .  $\Delta Q_{gs}(ii) = \min\{ Q_{gs,m}^{\max} -$   
 226  $Q_{gs,m}(ii), V_m^{\max} - V_{gs,m}(ii) \}$ ; If the gas node where the gas storage  $m$  is connected with P2G,  $\Delta Q_{P2G}(ii)$   
 227  $= Q_{P2G}^{\max} - Q_{P2G}(ii)$ , the effective redundancy  $\Delta Q(ii) = \min\{\Delta Q_{gs}(ii), \Delta Q_{P2G}(ii)\}$ ; else,  $\Delta Q(ii) = \Delta Q_{gs}(ii)$ .  
 228 Then, arrange  $\Delta Q$  in descending order;
- 229 d) According to the descending order,  $Q_{P2G}(ii)$  and  $Q_{gs,m}(ii)$  are adjusted successively until  $V_m(t) \geq V_m^{\min}$ ;
- 230 e) Update  $V_m(t)$ ;
- 231 f) If  $V_m(t) \geq V_m^{\max}$ , calculate  $\Delta V = V_m(t) - V_m^{\max}$ ;
- 232 g) For  $ii = 1:t$ , calculate the gas flow redundancy of gas storage  $m$  at time  $ii$ .  $\Delta Q_{gs}(ii) = \min\{ Q_{gs,m}(ii) -$   
 233  $Q_{gs,m}^{\min}, V_{gs,m}(ii) - V_m^{\min} \}$ ; If the gas node where the gas storage  $m$  is connected with P2G,  $\Delta Q_{P2G}(ii) =$   
 234  $Q_{P2G}(ii) - Q_{P2G}^{\min}$ , the effective redundancy  $\Delta Q(ii) = \min\{\Delta Q_{gs}(ii), \Delta Q_{P2G}(ii)\}$ ; else,  $\Delta Q(ii) = \Delta Q_{gs}(ii)$ .  
 235 Then, arrange  $\Delta Q$  in descending order;
- 236 h) According to the descending order,  $Q_{P2G}(ii)$  and  $Q_{gs,m}(ii)$  are adjusted successively until  $V_m(t) \leq V_m^{\max}$ ;
- 237 i) Update  $V_m(t)$ .

### 238 3. Case Studies Application

#### 239 3.1 Description of case studies

240 The hybrid electricity-natural gas energy systems shown in Figure 3 is composed by the revised  
 241 IEEE 39-bus power system [35] and Belgian high-calorific 20-node gas system [3]. The IEEE 39-bus  
 242 power network has 46 branches, 5 coal-fired units, 3 gas-fired units and 2 wind power units, where  
 243 the capacity of wind power units accounts for 35% of the total installed capacity of 3903 MW. The  
 244 Belgian high-calorific 20-node gas system has 24 pipelines, 2 gas wells, 3 gas storages and 2

245 compressors. The parameters of the power system are from [35,40] and the parameters of natural  
 246 gas system are from [3]. The revised parameters are shown in Table 1 and Table 2 (inflow of gas  
 247 storage is positive and outflow of gas storage is negative). Gas pressure limits of gas nodes are given  
 248 in Table 3. Power demand and gas demand are given in Table. 3. In addition, the theoretical  
 249 predicted wind power output is given in Figure 4. The efficiency of P2G process is taken as 64% [6].  
 250 Wind curtailment cost is set as 100 \$/MWh [47]. The short-term optimal dispatch for this hybrid  
 251 energy system is studied to illustrate the behavior of the proposed model, the adopted algorithm  
 252 and the proposed constraints handling methods in several case studies. These case studies are  
 253 simulated with a low level of initial line pack (0.5 Mm<sup>3</sup>). In addition, all the case studies are  
 254 implemented using MATLAB language programming.

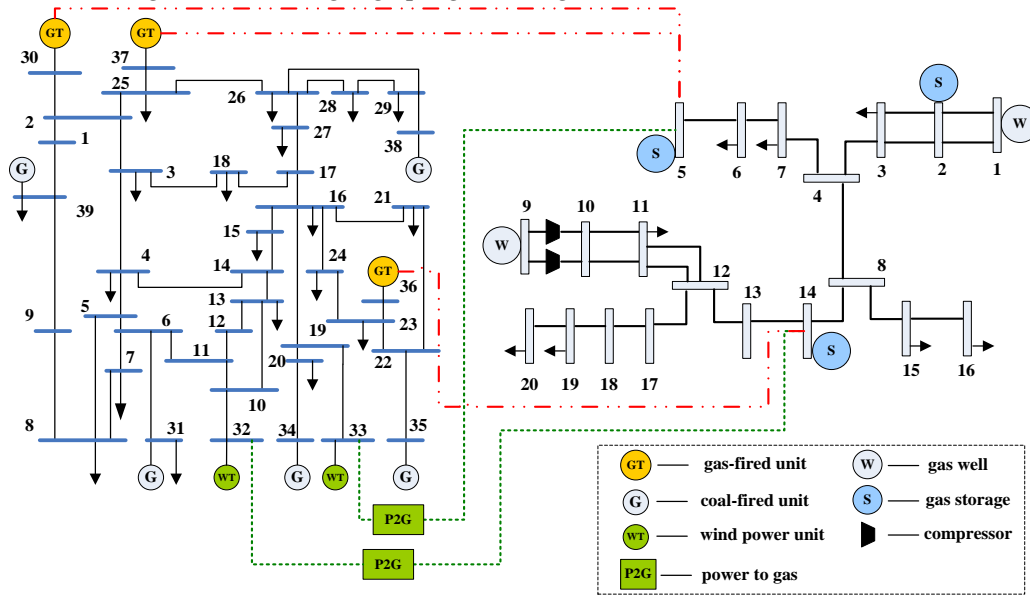


Figure 3. The hybrid electricity-natural gas energy systems

Table 1. Parameters of power units

Power units	$P_{max}/MW$	$P_{min}/MW$	Ramp up rate /MW/h	Ramp down rate/MW/h
Coal-fired unit 1	470	150	80	80
Coal-fired unit 2	470	135	80	80
Coal-fired unit 3	340	73	80	80
Coal-fired unit 4	300	60	50	50
Coal-fired unit 5	243	73	50	50
Gas-fired unit 1	260	0	260	260
Gas-fired unit 2	230	0	230	230
Gas-fired unit 3	220	0	220	220
Wind power unit 1	750	0	750	750
Wind power unit 2	620	0	620	620

Table 2. Parameters of gas storage

Gas storage	Initial	Max capacity	Min capacity	Max gas flow	Min gas flow
No.	capacity/Mm <sup>3</sup>	/Mm <sup>3</sup>	/Mm <sup>3</sup>	/Mm <sup>3</sup> /h	/Mm <sup>3</sup> /h
Gas Storage 1	1.5	3.5	0	0.35	-0.20
Gas Storage 2	2.0	4.5	0	0.45	-0.25
Gas Storage 3	1.5	3.5	0	0.35	-0.25

Table 3. Gas pressure limits of gas nodes

255  
256  
257

258

259

Node No.	1	2	3	4	5	6	7	8	9	10	11	12	13	14	15	16	17	18	19	20
$M_{\min}/\text{bar}$	30	30	30	30	10	10	30	30	50	50	30	30	30	30	15	15	25	25	15	15
$M_{\max}/\text{bar}$	100	100	100	80	80	80	80	70	70	77	70	70	70	70	70	70	70	70	70	70

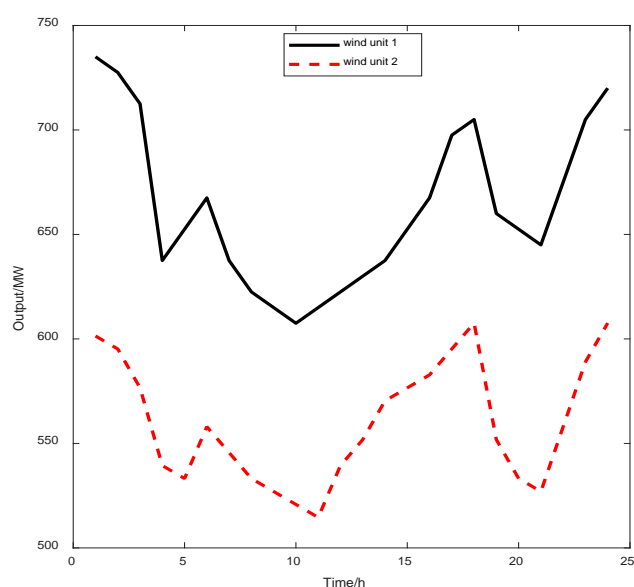
260

261

262

**Table 4.** Power demand and gas demand

Time/h	1	2	3	4	5	6	7	8	9	10	11	12
Power demand/MW/h	1272	1188	1104	960	1080	1320	1476	1584	1740	1776	1800	1860
Gas demand/ Mm <sup>3</sup> /h	1.03	0.97	0.92	0.98	0.99	1.03	1.23	1.45	1.79	1.83	1.74	1.61
Time/h	13	14	15	16	17	18	19	20	21	22	23	24
Power demand/MW/h	1680	1560	1320	1104	1416	1680	1800	2040	1860	1632	1344	1116
Gas demand/ Mm <sup>3</sup> /h	1.46	1.42	1.39	1.38	1.39	1.30	1.26	1.19	1.15	1.15	1.12	0.97



263

264

**Figure 4.** Predicted output of wind power units

### 265 3.2 Analysis of simulation results

266 The Newton-Raphson method is used to obtain the power flow. Trust region method and L-M  
 267 method are used to solve the non-linear equations to obtain the gas flow in natural-gas system,  
 268 respectively. Furthermore, MOBPSO [39-42] is used to optimize the multi-objective dispatch  
 269 problem of hybrid electricity-natural gas energy systems based on the established models  
 270 (1)(2)(3)(7)(12), the proposed flow chart (Figure 2.) and the proposed constraints handling methods.  
 271 The optimization results are shown in Table 5 and Table 6. And all the constraints are satisfied. The  
 272 comparisons of power output and gas flow among different case studies are given in Figure 5 and  
 273 Figure 6, respectively. Moreover, it can be found the different performance of trust region method  
 274 and L-M method from Figure 7 and Table 6. The wind power absorbed by P2G and the gas flow of  
 275 P2G are shown in Figure 8. The volume of gas storages is given in Figure 9. And the gas pressure of  
 276 each gas node can be found in Appendix A.

277 From the obtained results, it can be seen that power output, gas flow of gas wells, gas flow of  
 278 P2G, gas flow of gas storages, volume of gas storages and gas pressure of gas nodes all satisfy their

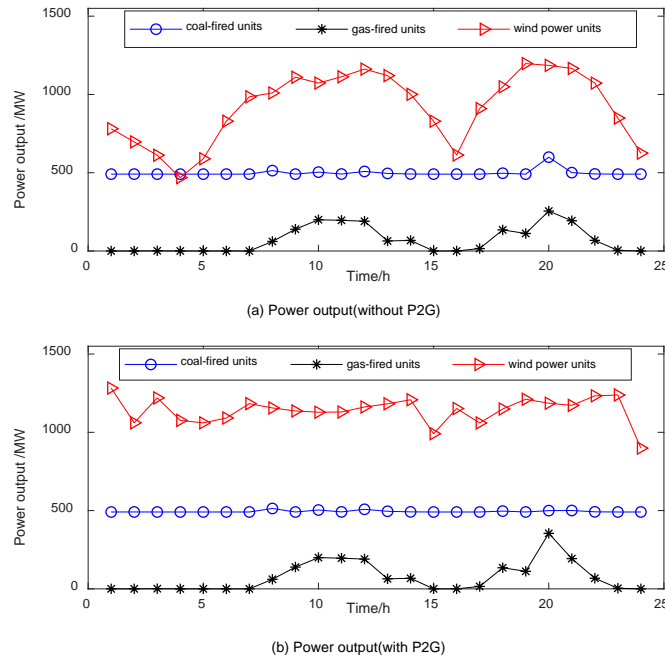
279 respective upper and lower bound constraints. Besides, the nodal gas flow balance equation is  
 280 satisfied. Moreover, power demand and power supply are balanced which can be drawn from the  
 281 calculated load loss rate  $L_p=6.37 \times 10^{-18}$ . Then the above results show that all the constraints are  
 282 satisfied using the proposed constraints handling methods.

283 **Table 5.** Optimization results of the power system

	Fuel cost (M\$)	SO <sub>x</sub> emission(ton)
Without P2G	1.080	38.193
With P2G	1.084	37.939

284 **Table 6.** Optimization results of the natural-gas system

	Cost of natural-gas /M\$	CO <sub>2</sub> emission /10 <sup>4</sup> ton	Rate of abandoned wind power	Operation cost of P2G /M\$	Absorbed CO <sub>2</sub> by the methanation process /10 <sup>4</sup> ton	Increased wind power by P2G /MWh
Without P2G						
Trust Region	0.741	5.791	24.85%	0	0	0
L-M	0.695	5.790	24.85%	0	0	0
With P2G						
Trust Region	0.732	5.727	6.71%	0.106	0.056	5321.66
L-M	0.685	5.491	4.04%	0.122	0.064	6104.48



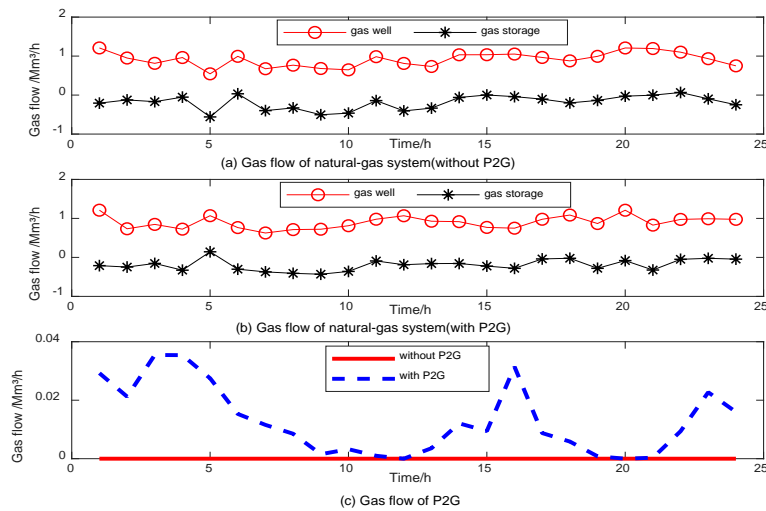
285  
 286 **Figure 5.** Comparison of power output without P2G and with P2G

287 3.2.1 Effects of P2G on the power system

288 (1) From Table 5 and Figure 5, it can be seen that the fuel cost of power system with P2G is a  
 289 little higher than that without P2G. At the hour 20, owing to the gas injection from P2G, the pipeline  
 290 pressure is higher than the maximum value, so the ‘gas demand management strategy’ is used and it  
 291 needs to increase the gas demand by increasing the output of gas-fired units connected with gas

292 node 5 and 14. Then, to guarantee the power load balance, the output of coal-fired units would be  
 293 reduced. Because the fuel cost of gas-fired units is higher than that of coal-fired units and the SO<sub>x</sub>  
 294 emissions of gas-fired units are lower than that of coal-fired units, it leads to increase of fuel cost  
 295 and decline of SO<sub>x</sub> emissions. And the SO<sub>x</sub> emissions are reduced by 0.254 ton. In addition, from  
 296 Figure 8, most abandoned wind power can be absorbed by P2G. During hours 3-5, P2G works at its  
 297 maximum value when the abandoned wind power is over the maximum capacity of P2G. Owing to  
 298 the P2G, the wind power output is much smoother and so is the output of coal-fired units, which is  
 299 propitious to the stability and reliability of the power system.

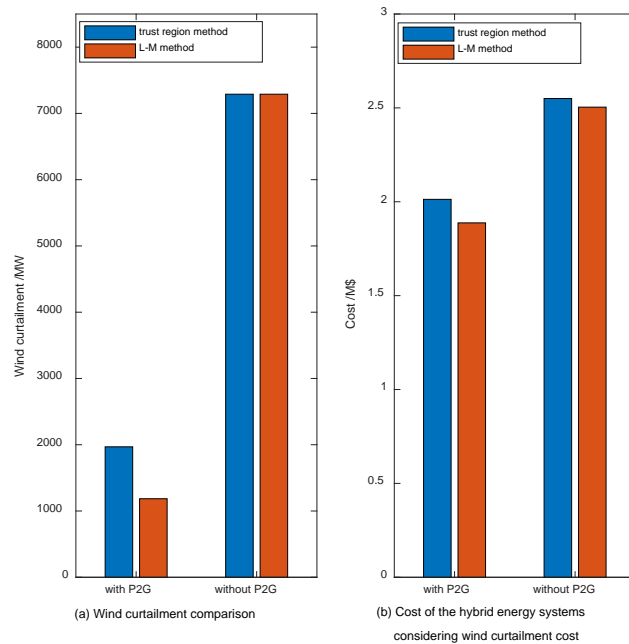
300 (2) From Table 6 and Figure 7(a), it is obvious that the rate of abandoned wind power is  
 301 declined from 24.85% to 6.71% (trust region) and from 24.85% to 4.04% (L-M), respectively; The  
 302 wind power output is increased by 5321.66MWh (trust region) and 6104.48MWh (L-M), respectively.



303

304

Figure 6. Comparison of gas flow without P2G and with P2G



305

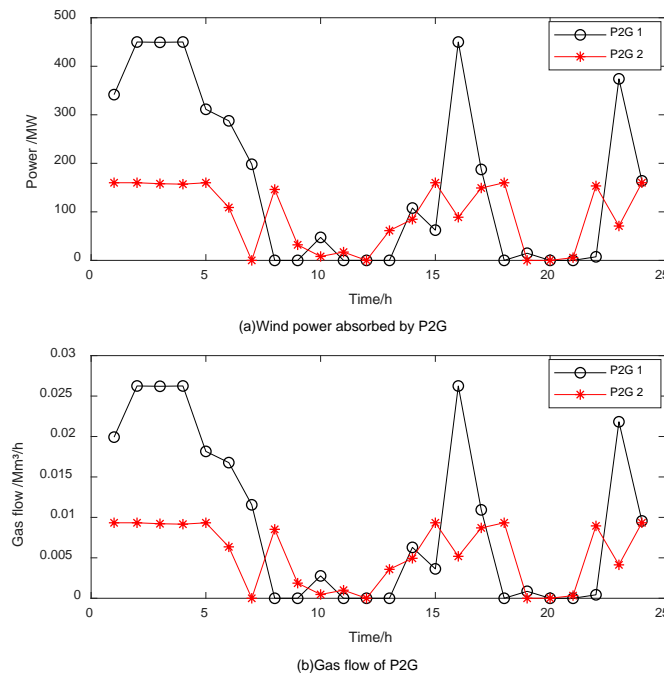
306

Figure 7. Results comparison of trust region method and L-M method

307 3.2.2 Effects of P2G on the natural-gas system

308 From Figure 6 and Figure 9, it's obvious that the gas flow of gas wells and gas storages is lower  
 309 when P2G is considered. Besides, the volume of gas storages with P2G is much larger than that

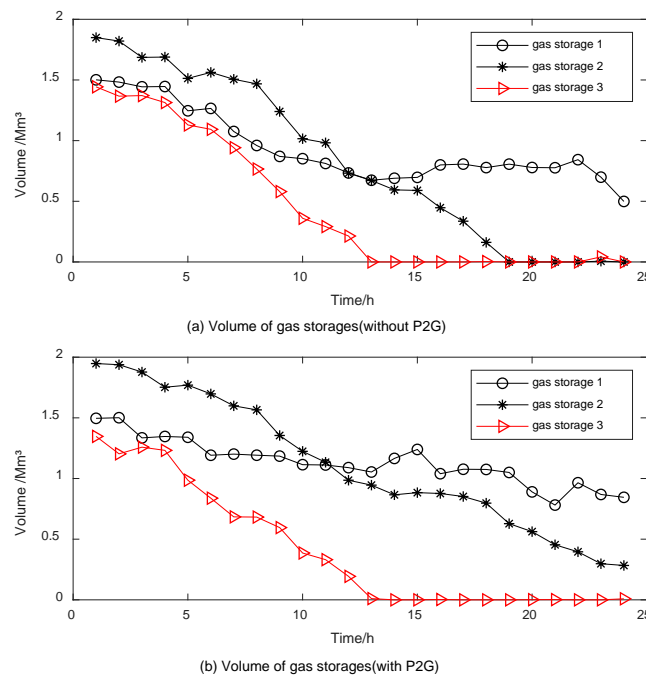
310 without P2G. This is because the economic, clean and low carbon energy converted by P2G from  
 311 wind power has the priority of use compared with that from natural gas network, which creates  
 312 considerable economic and environmental benefits for the integrated energy systems. The cost  
 313 benefit of P2G is evaluated in terms of the natural gas cost which it displaces. From Table 6, it can be  
 314 seen the gas cost is reduced by 9000 \$ (trust region) and 10000\$ (L-M), respectively; Moreover, the  
 315 environmental benefit of P2G in terms of CO<sub>2</sub> reduction and CO<sub>2</sub> absorbed in the P2G methanation  
 316 process is measured. The total CO<sub>2</sub> emissions are declined by 1200 ton (trust region) and 3630 ton  
 317 (L-M), respectively.



318

319

**Figure 8.** Wind power absorbed by P2G and the gas flow of P2G



320

321

**Figure 9.** Volume of gas storages without P2G and with P2G

### 322 3.2.3 Total cost reduction of the hybrid energy systems

323 The total cost of the hybrid electricity-natural gas energy systems including the wind power  
 324 curtailment cost is reduced by  $5.372 \times 10^5$  \$ (trust region) and  $6.165 \times 10^5$  \$ (L-M), which can be seen  
 325 from Figure 7(b).

326 It can be concluded that the proposed model, the proposed constraints handling methods are  
 327 effective and the feasibility of MOBHPSO algorithm for solving the multi-objective optimal dispatch  
 328 problem of the hybrid electricity-natural gas energy systems is indicated. Moreover, the trust region  
 329 method and L-M method are effective to solve the nonlinear gas flow problem. And it also can be  
 330 seen that the results obtained from L-M method is much better than those obtained from trust region  
 331 method.

## 332 4. Conclusion

333 This paper presented a multi-objective optimal dispatch model of the hybrid electricity-natural  
 334 gas energy systems coupled by P2G and gas turbines, in order to achieve the maximum of  
 335 low-carbon economic environmental benefits. The proposed model provides not only enhanced  
 336 flexibility as it easily handles bidirectional energy flow and guarantees global optimality, but also  
 337 considers the compressibility of gas, line pack of pipelines among other complicated system  
 338 characteristics. The nonlinear and non-convex functions of gas flow model are addressed by trust  
 339 region method and L-M method. And the L-M method has much better performance which can be  
 340 drawn from the simulation results. Moreover, the case studies simulation results show the feasibility  
 341 of MOBHPSO algorithm for solving the multi-objective optimal dispatch problem of the hybrid  
 342 electricity-natural gas energy systems and the effectiveness of proposed constraints handling  
 343 methods. The obtained results also illustrate that P2G can significantly benefit the operation of both  
 344 power system and natural gas system in smoothing power output, cutting down gas cost, reducing  
 345 CO<sub>2</sub> emissions and SO<sub>x</sub> emissions as well as avoiding wind curtailment. More specifically, the gas  
 346 cost is cut down up to 10000 \$, the total CO<sub>2</sub> emissions are declined up to 3630 ton and the SO<sub>x</sub>  
 347 emissions are reduced by 0.254 ton as well as the wind power curtailment is decreased up to 6104.48  
 348 MWh with the rate of abandoned wind power declined from 24.85% to 4.04%. Besides, the total cost  
 349 including wind power curtailment cost is reduced up to  $6.165 \times 10^5$  \$.

350 **Author Contributions:** Dr. Jing Liu proposed the optimization model and algorithms, carried out case studies,  
 351 completed the entire analysis and wrote this paper; Prof. Gareth Harrison gave essential and important advice  
 352 on the model of natural-gas system; Dr. Wei Sun gave some important suggestions on the calculation of gas  
 353 flow and revised this paper.

354 **Acknowledgments:** The authors would like to thank Dr. Carlos M. Correa-Posada who provided some  
 355 important data used for the case studies.

356 **Conflicts of Interest:** The authors declare no conflict of interest.

## 357 Appendix A

358 **Table A1.** Gas pressure of each gas node

Node No.	1	2	3	4	5	6	7	8	9	10
Hour 1	74.7469	73.8385	72.5356	56.7444	45.5189	41.0362	42.8709	43.8394	55.7467	61.3213
Hour 2	67.0635	66.5001	65.6495	55.1170	39.9237	38.1803	40.9818	45.8246	50.2401	55.2641
Hour 3	70.9782	70.6287	69.6258	56.8556	53.1330	46.9431	47.4426	40.3510	54.5096	59.9605
Hour 4	67.7032	67.1715	66.3961	57.2499	70.7133	54.9508	54.2037	42.9448	53.3986	58.7385
Hour 5	60.3126	59.8906	59.2212	51.7346	33.9220	33.5808	37.1390	46.9318	49.9918	54.9910
Hour 6	60.2348	60.0091	59.2823	51.2112	48.2071	40.7850	41.2236	44.1951	50.0255	55.0280
Hour 7	61.7065	61.2190	60.5111	52.7660	56.6407	46.2672	46.2665	44.8522	51.1059	56.2164
Hour 8	72.0210	71.2920	70.1714	55.5450	30.7629	30.7596	37.3143	40.5826	50.3482	55.3830

Hour 9	59.6538	59.2193	58.5192	50.4304	63.6206	46.3675	45.9280	38.7845	52.4694	57.7163
Hour 10	63.8376	63.4229	62.5894	52.8985	40.6647	38.5312	40.3515	45.1444	53.4969	58.8466
Hour 11	70.6866	69.9749	68.8971	54.9136	27.6230	27.5911	35.2202	41.7990	50.9478	56.0425
Hour 12	68.9173	68.3366	67.3818	55.2606	41.9605	38.5358	40.9826	43.4697	52.3659	57.6024
Hour 13	64.6456	64.1633	63.3132	52.9436	32.3582	31.5162	36.1046	44.7830	50.4011	55.4412
Hour 14	68.1243	67.1946	66.2050	53.6897	45.2849	40.2787	41.5617	39.2924	51.8961	57.0857
Hour 15	77.3472	76.3396	75.1040	58.2513	28.6262	28.7076	37.7480	40.5386	50.1422	55.1564
Hour 16	74.0179	73.6698	72.5552	57.3796	36.5834	35.4363	40.2615	40.3234	50.9462	56.0408
Hour 17	72.7026	71.9010	70.8103	56.1345	35.5315	34.6661	39.3576	39.7726	50.2135	55.2349
Hour 18	75.1341	74.3651	73.1955	57.2444	37.5240	36.4759	40.8464	38.1481	50.2537	55.2791
Hour 19	70.4893	69.9243	68.9806	56.8986	63.1603	51.1618	51.1398	38.1952	53.7179	59.0897
Hour 20	90.0790	89.4097	87.8955	66.0627	30.6166	32.7061	44.5817	38.5313	51.2693	56.3962
Hour 21	72.9250	72.4852	71.4642	57.2781	44.5136	41.6715	44.0290	38.2162	56.4074	62.0482
Hour 22	69.5078	68.3668	67.3470	53.8900	37.1964	35.8036	39.0643	38.5332	54.3579	59.7937
Hour 23	70.0484	69.6090	68.6537	56.6512	59.8959	49.6890	49.7032	40.4218	53.2979	58.6277
Hour 24	56.7456	56.3199	55.5790	46.7811	33.0590	31.2034	33.3676	38.3445	64.6311	71.0942
<b>Node No.</b>	<b>11</b>	<b>12</b>	<b>13</b>	<b>14</b>	<b>15</b>	<b>16</b>	<b>17</b>	<b>18</b>	<b>19</b>	<b>20</b>
Hour 1	54.1081	50.5855	46.0875	44.7456	35.3047	25.7453	49.7105	35.4170	26.1208	25.9488
Hour 2	51.7236	50.3445	47.8200	46.7134	37.8536	29.1582	49.9537	40.2191	31.2779	31.1271
Hour 3	54.3675	51.3623	45.1763	40.7143	31.6600	21.1181	51.0356	43.0089	35.4623	35.3304
Hour 4	53.8731	51.4255	46.4733	43.5065	34.3087	24.3816	51.1668	44.6069	37.9960	37.8745
Hour 5	51.9467	50.9341	49.0610	48.4082	39.0532	30.5918	50.7221	45.1699	39.1410	39.0242
Hour 6	51.3066	49.8506	46.9020	45.3095	36.2103	27.2829	49.6736	44.8413	39.1515	39.0360
Hour 7	52.2445	50.6172	47.4860	45.9142	36.8016	27.8913	50.4070	45.1037	39.3228	39.2076
Hour 8	50.8360	48.7091	44.1013	41.0575	31.8666	21.3437	48.5566	44.1770	38.6343	38.5179
Hour 9	52.3018	49.4738	43.5577	39.5966	29.3700	17.2155	49.2713	44.1255	38.3480	38.2301
Hour 10	54.3000	52.1931	48.2816	46.3746	36.7013	27.3680	51.9234	45.6230	39.5052	39.3897
Hour 11	51.6829	49.6546	45.2476	42.3900	33.2849	23.2977	49.4998	44.9943	39.3993	39.2845
Hour 12	52.9842	50.8287	46.5780	44.1992	35.0247	25.4320	50.6144	45.2823	39.5316	39.4170
Hour 13	51.7051	50.2120	47.2589	45.8176	36.6459	27.6235	50.0282	45.1247	39.4647	39.3501
Hour 14	51.9730	49.3827	43.7844	39.8147	30.3185	19.0701	49.2116	44.5565	38.9702	38.8546
Hour 15	50.5211	48.3266	43.7034	40.9399	31.3684	20.1573	48.1649	43.6773	38.0939	37.9760
Hour 16	51.1041	48.7023	43.7603	40.7302	31.1775	19.9426	48.5071	43.4549	37.6395	37.5197
Hour 17	50.4220	48.1032	43.2388	40.2295	30.5039	18.9170	47.9215	43.0252	37.1790	37.0577
Hour 18	50.1500	47.5764	42.0906	38.4792	28.4809	15.5972	47.3952	42.5038	36.6134	36.4903
Hour 19	53.1562	49.8808	43.1425	38.5692	28.3725	15.1925	49.6243	43.5000	37.2428	37.1207
Hour 20	51.1983	48.4743	42.5615	38.5943	28.7701	15.8577	48.2927	43.2795	37.3198	37.1984
Hour 21	55.6171	51.8483	44.0882	38.5362	28.4171	15.2929	51.5608	44.9563	38.6616	38.5433
Hour 22	54.1611	50.9718	44.0340	39.1087	28.7767	15.8746	50.7701	45.4186	39.5082	39.3929
Hour 23	53.3906	50.6155	44.7480	40.9330	31.0949	19.5983	50.4247	45.3936	39.6974	39.5833
Hour 24	63.3091	58.1787	47.7707	39.5037	28.7623	16.1240	57.7734	49.4686	43.0386	42.9313



359 **References**

- 360 1. Mazza, A.; Bompard, E.; Chicco, G. Application of power to gas technologies in emerging electrical  
361 systems. *Renewable Sustainable Energy Rev.* **2018**, *92*, 794–806. [DOI: 10.1016/j.rser.2018.04.072]
- 362 2. Hibbard, P. J.; Schatzki, T. The interdependence of electricity and natural gas: Current factors and future  
363 prospects. *Electricity J.* **2012**, *25*, 6–17. [DOI: 10.1016/j.tej.2012.04.012]
- 364 3. Correa-Posada, C. M.; Pedro Sánchez-Martín. Integrated power and natural gas model for energy  
365 adequacy in short-term operation. *IEEE Trans. Power Syst.* **2015**, *30*, 3347–3355.  
366 [DOI: 10.1109/TPWRS.2014.2372013]
- 367 4. Schiebahn, S.; Grube, T.; Robinius, M.; Tietze, V.; Kumar, B.; Stolten, D. Power to gas: technological  
368 overview, systems analysis and economic assessment for a case study in Germany. *Int. J. Hydrogen Energy*  
369 **2015**, *40*, 4285–4294. [DOI: 10.1016/j.ijhydene.2015.01.123]
- 370 5. Götz, M.; Lefebvre, J.; Mörs, F.; McDaniel Koch, A.; Graf, F.; Bajohr, S.; Reimert, R.; Kolb, T. Renewable  
371 power-to-gas: a technological and economic review. *Renew. Energy* **2016**, *85*, 1371–1390.  
372 [DOI: 10.1016/j.renene.2015.07.066]
- 373 6. Maroufmashat, A.; Fowler, M. Transition of future energy system infrastructure: through power-to-gas  
374 pathways. *Energies*, **2017**, *10*, 1089–1110. [DOI: 10.3390/en10081089]
- 375 7. Mukherjee, U.; Maroufmashat, A.; Narayan, A.; Elkamel, A.; Fowler, M. A stochastic programming  
376 approach for the planning and operation of a power to gas energy hub with multiple energy recovery  
377 pathways. *Energies* **2017**, *10*, 868–894. [DOI: 10.3390/en10070868]
- 378 8. Eveloy, V.; Gebreegziabher, T. A review of projected power-to-gas deployment scenarios. *Energies*  
379 **2018**, *11*, 1824–1875. [DOI: 10.3390/en11071824]
- 380 9. Clegg, S.; Mancarella, P. Integrated modeling and assessment of the operational impact of power-to-gas  
381 (P2G) on electrical and gas transmission networks. *IEEE Trans. Sustainable Energy* **2015**, *6*, 1234–1244.  
382 [DOI: 10.1109/TSTE.2015.2424885]
- 383 10. Department of Energy and Climate Change. The future of heating: meeting the challenge. HM  
384 Government, London, UK, 2013.
- 385 11. Ball, M. B.; Wietschel, M. *The hydrogen economy: opportunities and challenges*. Cambridge University Press:  
386 Cambridge, UK, 2009.
- 387 12. An, S.; Li, Q.; Gedra, T. W. Natural gas and electricity optimal power flow. Proceedings of IEEE PES  
388 Transmission and Distribution Conference and Exposition, Dallas, TX, USA, 7–12 September, 2003.  
389 [DOI: 10.1109/TDC.2003.1335171]
- 390 13. Chen, S.; Wei, Z. N.; Sun, G. Q.; Wang, D.; Sun, Y. H.; Zang, H. X.; Zhu, Y. Probabilistic energy flow  
391 analysis in integrated electricity and natural-gas energy systems. *Proc. CSEE* **2015**, *35*, 6331–6340. [DOI:  
392 10.13334/j.0258-8013.pcsee.2015.24.008]
- 393 14. Sun, G. Q.; Chen, S.; Wei, Z. N.; Chen, S.; Li, Y. C. Probabilistic optimal power flow of combined natural  
394 gas and electric system considering correlation. *Autom. Electr. Power Syst.* **2015**, *39*, 11–17. [DOI:  
395 10.7500/AEPS20150611006]
- 396 15. Osiadacz, A. J. *Simulation and Analysis of Gas Networks*. Gulf Publishing Company: USA, 1987.
- 397 16. Liu, C.; Shahidehpour, M.; Fu, Y.; Li, Z. Y. Security-constrained unit commitment with natural gas  
398 transmission constraints. *IEEE Trans. Power Syst.* **2009**, *24*, 1523–1536. [DOI: 10.1109/TPWRS.2009.2023262]
- 399 17. Geidl, M.; Andersson, Q. Optimal power flow of multiple energy carriers. *IEEE Trans. Power Syst.* **2007**, *22*,  
400 145–155. [DOI: 10.1109/TPWRS.2006.888988]
- 401 18. Qadrdan, M.; Wu, J. Z.; Jenkins, N.; Ekanayake, J. Operating strategies for a GB integrated gas and  
402 electricity network considering the uncertainty in wind power forecasts. *IEEE Trans. Sustainable Energy*  
403 **2014**, *5*, 128–138. [DOI: 10.1109/TSTE.2013.2274818]
- 404 19. Chaudry, M.; Jenkins, N.; Strbac, G. Multi-time period combined gas and electricity network optimization.  
405 *Electr. Power Syst. Res.* **2008**, *78*, 1265–1279. [DOI: 10.1016/j.epsr.2007.11.002]
- 406 20. Wang, W. L.; Wang, D.; Jia, H. J.; Chen, Z. Y.; Guo, B. Q.; Zhou, H. M.; Fan, M. H. Steady state analysis of  
407 electricity-gas regional integrated energy system with consideration of NGS network status. *Proc. CSEE*  
408 **2017**, *37*, 1293–1304. [DOI: 10.13334/j.0258-8013.pcsee.160250]
- 409 21. Odetayo, B.; Kazemi, M.; MacCormack, J.; Rosehart, W. D.; Zareipour, H.; Seifi, A. R. A chance  
410 constrained programming approach to the integrated planning of electric power generation, natural gas  
411 network and storage. *IEEE Trans. Power Syst.* **2018**, *33*, 6883–6893. [DOI: 10.1109/TPWRS.2018.2833465]

- 412 22. Guandalini, G.; Robinius, M.; Grube, T.; Campanari, S.; Stolten, D. Long-term power-to-gas potential from  
413 wind and solar power: a country analysis for Italy. *Int. J. Hydrogen Energy* **2017**, *42*, 13389-13406.  
414 [DOI: 10.1016/j.ijhydene.2017.03.081]
- 415 23. Liu, W. J.; Wen, F. S.; Xue Y. S. Power-to-gas technology in energy systems: current status and prospects of  
416 potential operation strategies. *J. Modern Power Syst. Clean Energy* **2017**, *5*, 439-450.  
417 [DOI: 10.1007/s40565-017-0285-0]
- 418 24. He, L. C.; Lu, Z. G.; Zhang, J. F.; Geng, L. J.; Zhao, H.; Li, X. P. Low-carbon economic dispatch for  
419 electricity and natural gas systems considering carbon capture systems and power-to-gas. *Appl. Energy*  
420 **2018**, *224*, 357-370. [DOI: 10.1016/j.apenergy.2018.04.119]
- 421 25. International Energy Agency. Prospects for hydrogen and fuel cell. International Energy Agency, Paris,  
422 France, 2005.
- 423 26. De Vries, H.; Florisson, O.; Tiekstra, G. Safe operation of natural gas appliances fueled with  
424 hydrogen/natural gas mixtures (progress obtained in the naturally-project). International Conference on  
425 Hydrogen Safety, San Sebastián, Spain, 11-13 September, 2007. [DOI: 10.1016/j.ijhydene.2006.10.018]
- 426 27. Dodds, P. E.; Demoullin, S. Conversion of the UK gas system to transport hydrogen. *Int. J. Hydrogen Energy*  
427 **2013**, *38*, 7189-7200. [DOI: 10.1016/j.ijhydene.2013.03.070]
- 428 28. Biegger, P.; Kirchbacher, F.; Medved, A. R.; Miltner, M.; Lehner, M.; Harasek, M. Development of  
429 honeycomb methanation catalyst and its application in power to gas systems. *Energies* **2018**, *11*, 1679-1695.  
430 [DOI: 10.3390/en11071679]
- 431 29. Li, Y.; Liu, W. J.; Zhao, J. H.; Wen, F. S.; Dong, C. Y.; Zheng, Y.; Zhang, R. Optimal dispatch of combined  
432 electricity-gas-heat energy systems with power-to-gas devices and benefit analysis of wind power  
433 accommodation. *Power Syst. Technol.* **2016**, *40*, 3680-3688. [DOI: 10.13335/j.1000-3673.pst.2016.12.008]
- 434 30. Clegg S.; Mancarella, P.; Integrated electrical gas network flexibility assessment in low-carbon  
435 multi-energy systems. *IEEE Trans. Sustainable Energy* **2016**, *7*, 718-731. [DOI: 10.1109/TSTE.2015.2497329]
- 436 31. Ye, J.; Yuan, R. X. Integrated natural gas, heat, and power dispatch considering wind power and  
437 power-to-gas. *Sustainability* **2017**, *9*, 1-16. [DOI: 10.3390/su9040602]
- 438 32. Li, G. Q.; Zhang, R. F.; Jiang, T. security-constrained bi-level economic dispatch model for integrated  
439 natural gas and electricity systems considering wind power and power-to-gas process. *Appl. Energy* **2017**,  
440 *194*, 696-704. [DOI: 10.1016/j.apenergy.2016.07.077]
- 441 33. Guandalini, G.; Campanari, S.; Romano, M. C. Power-to-gas plants and gas turbines for improved wind  
442 energy dispatchability: energy and economic assessment. *Appl. Energy* **2015**, *147*, 117-130.  
443 [DOI: 10.1016/j.apenergy.2015.02.055]
- 444 34. Chen, Z. Y.; Wang, D.; Jia, H. J.; Wang, W. L.; Guo, B. Q.; Qu, B.; Fan, M. H. Research on optimal day-ahead  
445 economic dispatching strategy for microgrid considering P2G and multi-source energy storage system.  
446 *Proc. CSEE* **2017**, *37*, 3067-3077. [DOI: 10.13334/j.0258-8013.pcsee.161017]
- 447 35. Wei, Z. N.; Zhang, S. D.; Sun, G. Q.; Zang, H. Y.; Chen, S.; Chen, S. Power-to-gas considered peak load  
448 shifting research for integrated electricity and natural-gas energy systems. *Proc. CSEE* **2017**, *37*, 4601-4609.  
449 [DOI: 10.13334/j.0258-8013.pcsee.161361]
- 450 36. He, C.; Liu, T. Q.; Wu, L.; Shahidepour, M. Robust coordination of interdependent electricity and natural  
451 gas systems in day-ahead scheduling for facilitating volatile renewable generations via power-to-gas  
452 technology. *J. Modern Power Syst. Clean Energy* **2017**, *5*, 375-388. [DOI: 10.1007/s40565-017-0278-z]
- 453 37. Shu, K. G.; Ai, X. M.; Fang, J. K.; Yao, W.; Chen, Z.; He, H. B.; Wen, J. Y. Real-time subsidy based robust  
454 scheduling of the integrated power and gas system. *Appl. Energy* **2019**, *236*, 1158-1167.  
455 [DOI: 10.1016/j.apenergy.2018.12.054]
- 456 38. Qu, K. P.; Zheng, B. M.; Yu, T.; Li, H. F. Convex decoupled-synergetic strategies for robust multi-objective  
457 power and gas flow considering power to gas. *Energy* **2019**, *168*, 753-771.  
458 [DOI: 10.1016/j.energy.2018.11.083]
- 459 39. Liu, J.; Luo, X. J. Environmental economic dispatching adopting multi-objective random black-hole  
460 particle swarm optimization algorithm. *Proc. CSEE* **2010**, *30*, 105-111. [DOI:  
461 10.13334/j.0258-8013.pcsee.2010.34.013]
- 462 40. Liu, J.; Luo, X. J. Short-term optimal environmental economic hydrothermal scheduling based on handling  
463 complicated constraints of multi-chain cascaded hydropower station. *Proc. CSEE* **2012**, *32*, 27-35. [DOI:  
464 10.13334/j.0258-8013.pcsee.2012.14.006]

- 465 41. Liu, J.; Luo, X. J. Optimal economic emission hydrothermal scheduling using a novel algorithm based on  
466 black hole theory and annual profit analysis considering fuel gas desulphurization. 1st International IET  
467 Renewable Power Generation Conference, Edinburgh, UK, 6-8 September, 2011.  
468 [DOI: 10.1049/cp.2011.0171]
- 469 42. Liu, J.; Lu, Q. W.; Liu, Y. Optimal capacity allocation of hybrid wind-solar-battery power system  
470 containing electric vehicles. 5th International IET Renewable Power Generation Conference, London, UK,  
471 21-22 September, 2016.
- 472 43. Byrd, R.H.; Gilbert, J. C.; Nocedal, J. A trust region method based on interior point techniques for  
473 nonlinear programming. *Math. Program.* **2000**, *89*, 149-185. [DOI: 10.1007/PL00011391]
- 474 44. Mohamed Abdelmageed Abdelaziz, M.; Farag, H. E.; El-Saadany, E. F.; Mohamed, Y. A. I. A novel and  
475 generalized three-phase power flow algorithm for islanded microgrids using a newton trust region  
476 method. *IEEE Trans. Power Syst.* **2013**, *28*, 190-201. [DOI: 10.1109/TPWRS.2012.2195785]
- 477 45. Wilamowski, B. M.; Yu, H. Improved computation for Levenberg-Marquardt training. *IEEE Trans. Neural*  
478 *Networks* **2010**, *21*, 930-937. [DOI: 10.1109/TNN.2010.2045657]
- 479 46. Kanzowa, C.; Yamashitab, N.; Fukushima, M. Levenberg-Marquardt methods with strong local  
480 convergence properties for solving nonlinear equations with convex constraints. *J. Comput. Appl. Math.*  
481 **2004**, *172*, 375-397. [DOI: 10.1016/j.cam.2004.02.013]
- 482 47. Zheng, J.; Wen, F. S.; Li, L.; Wang, K.; Gao, C. Transmission system expansion planning considering  
483 combined operation of wind farms and energy storage systems. *Autom. Electr. Power Syst.* **2013**, *37*,  
484 135-142. [DOI: 10.7500/AEPS201206068]